

of the materials we used for the synthesis of the crystals showed that the maximum concentration of impurity ions, excluding those mentioned above, was ≤ 0.01 of the $^{143}\text{Nd}^{+3}$ concentration. Interactions with non-Kramers magnetic ion impurities, if they are occurring, are not reflected in a deviation of the temperature dependence of our observed Raman rates from the predicted T^9 dependence. The problem is being further investigated.

*This research has been supported by the National Science Foundation.

†We acknowledge the general support of the Materials Research Laboratory by the National Science Foundation.

‡Enrico Fermi Postdoctoral Fellow, 1971–1972.

¹C. D. Jeffries, *Dynamic Nuclear Orientation* (Interscience, New York, 1963).

²A. Abragam and B. Bleaney, *Electron Paramagnetic Resonance of Transition Metal Ions* (Clarendon Press, Oxford, England, 1970), Chap. 10.

³R. C. Mikkelsen and H. J. Stapleton, *Phys. Rev.* **140**,

A1968 (1965).

⁴B. W. Mangum and R. P. Hudson, *J. Chem. Phys.* **44**, 704 (1966).

⁵E. R. Bernstein and D. R. Franceschetti, *Phys. Rev. B* **6**, 1654 (1972).

⁶E. R. Bernstein and D. R. Franceschetti, *Phys. Rev. B* **9**, 3678 (1974).

⁷L. E. Erickson, *Phys. Rev.* **143**, 295 (1966).

⁸Dr. Bernstein and Dr. Franceschetti have most generously made available to us their revised calculations of the direct phonon-exchange plus Raman relaxation rates. In Ref. 5 it is erroneously stated that in zero external field a T^7 temperature dependence should be observed for the Raman relaxation rate (see p. 1661). In footnote 30 of Ref. 6 this statement is corrected and the T^9 dependence is correctly given. They have repeated the calculations for $^{143}\text{Nd}^{+3}$ in LaCl_3 using the corrected theory and it is to these revised calculations that we refer in this paper.

⁹C. A. Hutchison, Jr., and E. Wong, *J. Chem. Phys.* **29**, 754 (1958).

¹⁰A. M. Prokhorov and V. B. Fedorov, *Zh. Eksp. Teor. Fiz.* **46**, 1937 (1964) [*Sov. Phys. JETP* **19**, 1305 (1964)].

¹¹K. L. Brower, H. J. Stapleton, and E. O. Brower, *Phys. Rev.* **146**, 233 (1966).

Molecular Motion Anisotropy as Reflected by a "Pseudosolid" Nuclear Spin Echo: Observation of Chain Constraints in Molten *cis*-1, 4-Polybutadiene

J. P. Cohen-Addad and R. Vogin

Laboratoire de Spectrométrie Physique associé au Centre National de la Recherche Scientifique, Université Scientifique et Médicale de Grenoble, 38041 Grenoble Cédex, France

(Received 12 June 1974)

A nuclear spin echo ("pseudosolid echo") analogous to a "solid echo" is predicted to be observed even within the motional-narrowing approximation, whenever the molecular motion symmetry gives rise to a nonzero average dipolar spin coupling. It is considered as a new characterization of molecular motion anisotropy. New features are discussed. They are well illustrated by "pseudosolid echoes" observed, for the first time, on protons bound to long chains in a molten polymer system. Echoes are shown to reflect chain constraints.

We report a set of new properties related to a nuclear "pseudosolid echo" which is contrasted to the dipolar echo observed on a wide variety of solids.^{1,2} By using a model, the "pseudosolid echo" is described within the motional-narrowing approximation. It is shown to be observed on spin systems bound to molecules undergoing fast anisotropic motions which do not average tensorial spin couplings to zero. This nonzero component plays a crucial role in the spin dynamics. Contrary to the solid echo, the echo maximum does not occur at twice the pulse spacing exactly; it does not rise to the full free-induction-decay

amplitude. To distinguish carefully the "pseudosolid echo" from more familiar spin echoes of Hahn,³ field-gradient effects are also discussed.

The anisotropy effect of a fast molecular motion upon the NMR signal is conveniently described by using the following model. Consider a single proton pair whose proton-proton vector, \vec{b} , has a constant length and is supposed to undergo anisotropic rotation in space. The dipolar energy, \mathcal{H}_D , of the two spin- $\frac{1}{2}$ protons is the only spin coupling which is presently taken into consideration. As a result of the anisotropic motion, the time average of the dipolar energy, $\overline{\mathcal{H}}_D$, is sup-

posed to be different from zero. The spin dynamics is considered in the motional-narrowing approximation; however, $\overline{\mathcal{H}}_D$ may be of the order of magnitude of the spin-spin relaxation time. Since the singlet state of the two-spin system is not involved in the spin dynamics, the density matrix is defined by using the triplet-state basis ($I=1$) only. To the first order of perturbation with respect to $\overline{\mathcal{H}}_D$, the general time evolution of the density matrix is shown to obey the following set of equations⁴:

$$\begin{aligned} d\rho_{1,0}/dt &= \rho_{1,0}(-i\delta + i\Delta - 1/T) - \rho_{0,1}/\theta \\ &= (d\rho_{0,1}/dt)_{c.c.}, \end{aligned} \quad (1)$$

$$\begin{aligned} d\rho_{0,-1}/dt &= \rho_{0,-1}(-i\delta - i\Delta - 1/T) - \rho_{1,0}/\theta \\ &= (d\rho_{0,-1}/dt)_{c.c.}, \end{aligned} \quad (2)$$

where $T^{-1} = (9\gamma^4\hbar^2/32)[J_{2,2}(2\omega_0) + J_{0,0}(0) + 6J_{1,1}(\omega_0)]$ and $\theta^{-1} = (9\gamma^4\hbar^2/8)J_{1,1}(\omega_0)$ with $J_{\alpha,\alpha}$ the usual spectral densities.⁵ $\Delta = (3\gamma^2\hbar/4b^3)\langle 1 - 3\cos^2\theta \rangle_t \neq 0$ is a time average over all orientations of \vec{b} with respect to the steady magnetic field; Δ should be averaged to zero in times of the order of 1 sec or greater.

The above equations are defined in the frame $OXYZ$, rotating at the proton Larmor frequency, ω_0 . The space inhomogeneity of the steady magnetic field is characterized by a distribution function $g(\delta)$; δ measures the frequency deviation from ω_0 . In the frame $OXYZ$, we characterize a rf pulse, $\xi(\alpha)$, by the angle, ξ , and the axis direction, α ($\alpha = x$ or y), of the magnetization rotation induced by the rf field. A two-pulse sequence is defined as $[\xi(\alpha), \tau, \xi'(\alpha')]$; τ is the pulse spacing. Three types of pulse sequences may be used to characterize unambiguously the observation of a dipolar echo on a conventional solid spin system¹: $\Sigma_1 \equiv [\frac{1}{2}\pi(x), \tau, \frac{1}{2}\pi(y)]$, $\Sigma_2 \equiv [\frac{1}{2}\pi(y), \tau, \frac{1}{2}\pi(y)]$, and $\Sigma_3 \equiv [\frac{1}{2}\pi(x), \tau, \pi(y)]$. The sequence Σ_1 is expected to give rise to a "solid echo," while Σ_2 and Σ_3 must not change the transverse-magnetization time evolution. The same pulse sequences are now applied to the present model and the resulting signals are analyzed. The transverse-magnetization time evolution following a $\frac{1}{2}\pi(x)$ pulse is found to be

$$M_x^0(t) = 0, \quad M_y^0(t) = (\gamma\hbar/2)\langle S(t)G(t)\Gamma(t) \rangle, \quad (3)$$

where

$$S(t) = \cosh(\Omega t) - (\theta^{-1}/\Omega) \sinh(\Omega t), \quad (4)$$

$$\Gamma(t) = (\hbar\omega_0/kT) \exp(-t/T), \quad (5)$$

with $\Omega^2 = \theta^{-2} - \Delta^2$ and $G(t) = \int g(\delta) \cos(\delta t) d\delta$. θ^{-1}

plays a crucial role in the spin dynamics, since according to its relative amplitude compared with that of Δ , the signal may or may not oscillate. The angular brackets indicate a powder average over all orientations of \vec{b} throughout the whole sample.

Equations (1) and (2) lead to the following transverse-magnetization time evolution:

$$\begin{aligned} M_y^1(t) &= \langle \Gamma(t)[S(t) + E(t, \tau)] \rangle \\ &\quad \times [G(t - 2\tau) + G(t)]/2, \end{aligned} \quad (6)$$

$$\begin{aligned} M_x^2(t) &= \langle \Gamma(t)[S(t) + E(t, \tau)] \rangle \\ &\quad \times [-G(t - 2\tau) + G(t)]/2, \end{aligned} \quad (7)$$

and

$$M_y^3(t) = \langle \Gamma(t)S(t) \rangle G(t - 2\tau), \quad (8)$$

corresponding to pulse sequences Σ_1 , Σ_2 , and Σ_3 , respectively;

$$E(t, \tau) = \{ \cosh(\Omega t) - \cosh[\Omega(t - 2\tau)] \} \Delta^2 / \Omega^2. \quad (9)$$

On close inspection of Eqs. (6)–(8), two new striking features are perceived. First, even in the absence of any field inhomogeneity a spin echo is expected to be observed; it is described by $M_y^1(t)$. The transverse magnetization as detected along the OY direction corresponds to the free decay $M_y^0(t)$ plus an additional signal which we shall call a "pseudosolid echo"; its amplitude is strictly related to the presence of a nonzero average dipolar coupling. Furthermore, as in the classical solid-spin-system case, no spin echo is expected to be observed after the pulse sequences Σ_2 or Σ_3 . However, the main difference between the "pseudosolid echo" and the classical one comes from the presence of a dissipative term $\Gamma(t)$ and also from the structure of the signal $E(t, \tau)$ [Eq. (9)]. The echo maximum is not expected to occur necessarily at $t = \tau$; the maximum amplitude does not rise to the full free-induction-decay amplitude.

The other feature corresponds to the case where the field-inhomogeneity effect is stronger than the free-induction decay. In this case, and for τ large enough, $M_y^1(t) = -M_x^2(t)$. In other words, just as in ordinary liquids [$\Delta = 0$ in Eqs. (6) and (7)], the two spin echoes have equal absolute intensities although a nonzero average dipolar coupling is involved in the spin dynamics. The origin of this surprising effect comes from the presence of a strong field inhomogeneity which induces a complete symmetry between the OX and OY directions, in the rotating frame. However, the

main difference between the "pseudosolid echo" and echoes observed on ordinary liquids comes from the comparison of amplitudes of echoes following pulse sequences Σ_1 (or Σ_2) with those of echoes following pulse sequences Σ_3 . The ratio

$$\psi(2\tau) = M_y^1(2\tau) / M_y^3(2\tau) \tag{10}$$

must be equal to $\frac{1}{2}$ in ordinary liquids [$\Delta = 0$, in Eq. (6)], whereas it is expected to be always higher than $\frac{1}{2}$ according to the present model.

This property permits the definition of the following experimental procedure to demonstrate conveniently the presence of a nonzero average dipolar coupling in any spin system. It is only necessary to perform the pulse sequences Σ_1 and Σ_3 , in the presence of a field gradient strong enough, and to observe the deviation of the ratio $\psi(2\tau)$ from $\frac{1}{2}$.

To measure the degree of anisotropy which characterizes the molecular motion under observation, it may be of interest to define a parameter directly related to the nonzero average dipolar coupling. Consider the normalized function

$$\eta(t, \tau) = [M_y^1(t) + M_x^2(t) - M_y^0(t)] / M_y^0(0); \tag{11}$$

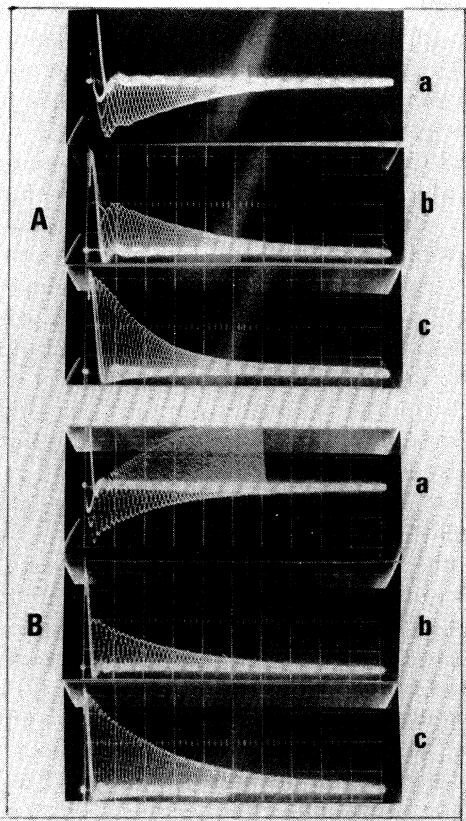


FIG. 1. Pulse sequences Σ_1 (curve a), Σ_2 (curve b), and Σ_3 (curve c) applied (A) to a molten polymer system and (B) to liquid water.

this function is easily drawn from experiments, by using the pulse sequences Σ_1 and Σ_3 . Notice that $\eta(\tau, \tau) = 0$ and that

$$S(\tau) = (d\eta/dt)_{t=\tau} = 2\langle(\Delta^2/\Omega)G(\tau) \sinh(\Omega\tau) \times \exp(-\tau/T)\rangle. \tag{12}$$

As will be shown below, $S(\tau)$ is a conveniently derived experimental parameter; it can be plotted against the pulse spacing τ . The slope $\xi = (dS/d\tau)_{\tau=0}$ gives the mean-square value of Δ , over all orientations in the sample:

$$\xi = 2\langle\Delta^2\rangle = (9\gamma^4\hbar^2/20b^6)\langle(3 \cos^2\theta - 1)^2\rangle_t. \tag{13}$$

ξ is directly related to the presence of nonzero average dipolar coupling.

The above properties are well illustrated by observing the proton signal on a molten polymer system of high molecular weight (4×10^5): *cis*-1, 4-polybutadiene. The transverse-magnetization free decay is observed to spread over a few milliseconds; the spin-lattice relaxation rate is found to be 6.2 sec^{-1} at room temperature. By taking into consideration, on the one hand, the spin density in this system (identical to that in liquid water, for example) and on the other hand the time range of the free-induction decay, it is easily seen that a motional-narrowing effect must characterize the proton magnetic signal whatever the exact nature of the monomer unit motion (presumably, semirotations and torsional oscillations). Furthermore, the great length of the chains gives rise to entanglements which prevent

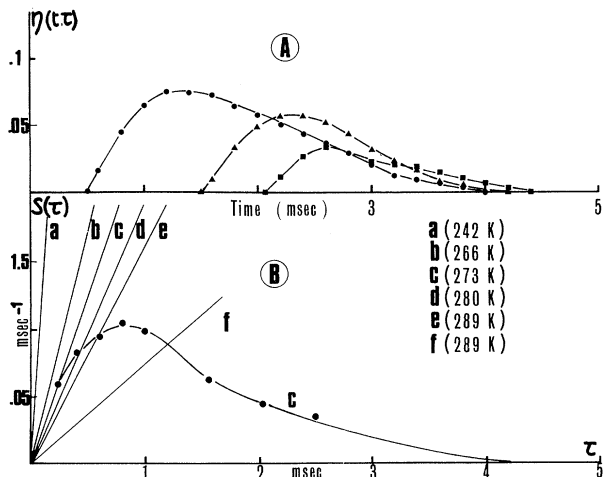


FIG. 2. (A) The function $\eta(t, \tau)$ corresponding to several τ values, at room temperature. (B) Initial slopes, ξ , corresponding to several temperatures (curves a-e). Curve c illustrates completely an $S(\tau)$ function. Curve f corresponds to a partly diluted polymer system.

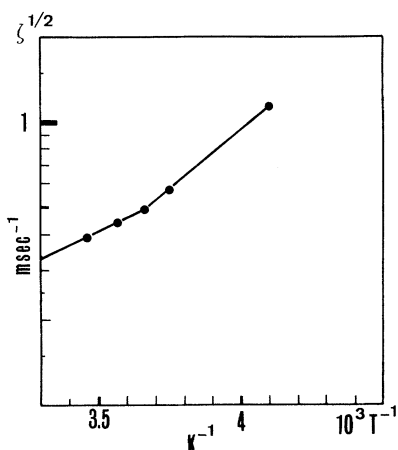


FIG. 3. The parameter $\zeta^{1/2}$ as a temperature function.

the chains from undergoing isotropic rotations (except in highly diluted solutions). The entanglement coupling plays a crucial role in chain fluctuations which govern viscoelastic properties of molten polymers⁶; however it is not easily observed directly. One of the purposes of the present Letter is to show that the observation of a "pseudosolid echo" gives a direct evidence for constraints exerted on chains. The *cis*-1,4-polybutadiene monomer unit consists of proton pairs ($-\text{CH}_2-\text{CH}=\text{CH}-\text{CH}_2$)_n; the melting point is 272 K. The dipolar interaction is the most important spin coupling. Figure 1(A) demonstrates the presence of nonzero average dipolar coupling in the molten polymer system, by using the pulse sequences Σ_1 , Σ_2 , and Σ_3 [$\psi(2\tau) > \frac{1}{2}$, Eq. (10)]; for comparison the same pulse sequences are applied to liquid water (with some paramagnetic impurities for convenience), at room temperature [Fig. 1(B)]; the ratio $\psi(2\tau)$ is found to be rigorously equal to $\frac{1}{2}$. The normalized function $\eta(t, \tau)$ derived from a series of experiments performed on the polymer system, at room temperature, is plotted as a function of τ , in Fig. 2(A). Also, one of the curves $S(\tau)$ is represented in Fig. 2(B), curve *c*, and corresponds to 273 K. Initial slopes, ζ , corresponding to several temperatures above

and below the polymer melting point are also presented in Fig. 2(B), curves *a-e*; ζ is found to increase when the temperature is lowered (Fig. 3). The variation of $\zeta^{1/2}$ must be related to thermal effects and also to the crystallization process. Most molten polymers are known to crystallize to a small extent, which depends on the cooling temperature, i.e., upon the crystallization rate.⁷ For the present polymer, the maximum extent (about 10%) has been observed at 245 K; the crystallization process is still very slow and quite negligible at 266 K.⁸ Crystallites must be considered as additional constraints exerted on chains. Correspondingly, the free-induction decay was observed to be very short at 245 K (spread over 800 μsec) and the "pseudosolid echo" was very sharp. Since the entanglement of network strands is known to be lowered upon the addition of a good solvent,⁹ it was of interest to observe the "pseudosolid echo" on a polymer-solvent system, at room temperature. The corresponding parameter, ζ , is shown in Fig. 2(B), curve *f*; as expected, ζ is found to be much smaller than that derived from the pure polymer system, at room temperature.

Finally, we must emphasize that experimental results corresponding to small molecules like benzene are found to be actually analogous to those observed on polymer chains; they will be published later.

¹P. Mansfield, Phys. Rev. **137**, A961 (1965).

²J. G. Powles and P. Mansfield, Phys. Lett. **2**, 58 (1962).

³E. L. Hahn, Phys. Rev. **80**, 500 (1950).

⁴J. P. Cohen-Addad, J. Chem. Phys. **60**, 2440 (1974).

⁵A. Abragam, *Principles of Nuclear Magnetism* (Oxford Univ. Press, London, 1961).

⁶J. P. Ferry, *Viscoelastic Properties of Polymers* (Wiley, New York, 1970), 2nd ed.

⁷L. Mandelkern, *Crystallization of Polymers* (McGraw-Hill, New York, 1964).

⁸L. E. Alexander, *X-Ray Diffraction Methods in Polymer Science* (Interscience, New York, 1969).

⁹F. N. Kelly and F. Bueche, J. Polym. Sci. **50**, 549 (1961).

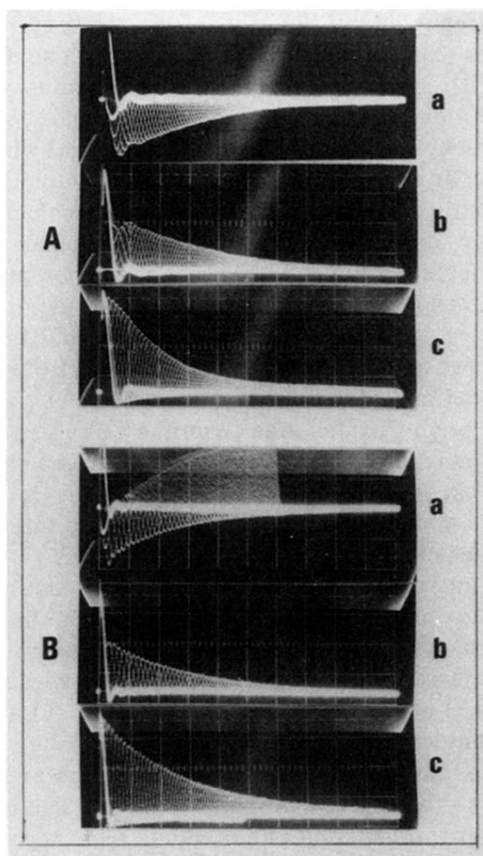


FIG. 1. Pulse sequences Σ_1 (curve *a*), Σ_2 (curve *b*), and Σ_3 (curve *c*) applied (A) to a molten polymer system and (B) to liquid water.